Strong plastic deformation and softening of fast colliding nanoparticles

Yoichi Takato* and Surajit Sen
Department of Physics, The State University of New York at Buffalo, Buffalo, New York 14260-1500, USA

Jeremy B. Lechman
Sandia National Laboratories, Albuquerque, New Mexico 87185, USA

(Received 17 June 2013; published 17 March 2014)

Nanoparticles, with sizes ranging between 1 and $\sim 10^2$ nm, show dynamical properties distinctly different than those of bulk materials. Due to their large surface area to volume ratio, their properties often depend on length scales. We investigate the size and the collision velocity ($v_{\rm coll}$) dependence of the coefficient of restitution (COR) for nanoparticles made of a face-centered cubic lattice of Lennard-Jones atoms via nonequilibrium molecular dynamics simulations. A sharp crossover between elastic collision and plastic collision occurs when $v_{\rm coll} = v_Y$, where v_Y is the size-dependent yield velocity. For high-collision velocities the COR $\sim v_{\rm coll}^{-\alpha}$, $\alpha \sim 1$. This result is in agreement with recent small system simulations and with experiments and is distinct from the elasticity-theory-based result for COR for inelastic collisions which behaves as $v_{\rm coll}^{-\alpha}$, with $\alpha = \frac{1}{4}$. We find that the size-dependent critical v_Y approaches the theoretical constant value for macroscopic spheres as our particle sizes grow. Possible insights into the origins of $\alpha \sim 1$ and the size dependence of the yield velocity are suggested. The work also suggests that sufficiently fast moving nanoparticles traveling through vacuum could be sticky and hence could be of potential interest in many applications.

DOI: 10.1103/PhysRevE.89.033308 PACS number(s): 36.40.−c, 45.50.Tn, 62.20.F−, 62.25.−g

I. INTRODUCTION AND BACKGROUND

The coefficient of restitution (COR), originally introduced by Newton [1], concerns the dynamical process of collision between two elastic bodies. It quantifies, in a coarse-grained way, the loss of kinetic energy in the observed degrees of freedom due to the simultaneous interactions of many unobserved degrees of freedom. Hence, the COR between an object and a rigid wall is defined as the ratio of the object's velocity after collision to the velocity prior to collision.

Collision phenomena have been extensively studied. For example, understanding the role of collisions in granular flow is crucial to the study of the dynamics that determines the flow patterns in fluidized beds [2]. In astrophysics, collisional processes influence the growth of dust aggregates and the formation of protoplanetary disks [3]. Nanoscale collisions are used to probe the chemical composition of nanoparticles [4]. Many studies that describe the collision between two macroscopic elastic objects have been reported. A nondissipative and nonadhesive macroscopic model to describe the collision of an elastic object is typically based on the Hertz contact law, which describes a highly nonlinear force-displacement behavior of two spherical elastic bodies as they come into intimate contact [5].

When two elastic solid spheres collide gently, elastic energy initially gets stored during the loading process and is subsequently released during the unloading process. There is no net energy loss in the loading-unloading sequence associated with the collision and thus the COR is unity. However, when the collision is at a high enough velocity, the center-of-mass motion and the atomic scale structure and dynamics become related. Hence the dependence of the COR on the collision velocity ends up being very different than the elasticity-theory-based result. This study focuses on the dynamical processes associated with collision at both the center-of-mass and molecular levels by considering particles that are sufficiently small.

Let us first briefly review the history of studies of COR for the elastic regime collisions of macroscopic spheres which repel upon contact according to the Hertz law [5]. A macroscopic model for sphere-sphere collisions allowing for energy dissipation can be derived by assuming that the spheres are composed of viscoelastic materials [6]. Viscoelastic collisions involve a relative-velocity-dependent term in the interaction potential and result in energy dissipation. Several other models incorporate dissipation mechanisms that yield a dependence of the COR on collision velocity, $v_{\rm coll}$ (see Ref. [7]). The viscoelastic Hertz models yield $1 - e \propto v_{\rm coll}^{1/5}$, e being the COR, which is in good agreement with the COR obtained via experiments [6]. A widely used grain-grain interaction model is due to Johnson-Kendall-Roberts (JKR) [8]. This model incorporates the adhesive surface energy at the contacting surfaces. The adhesive energy is important for a small object because the ratio of surface area to volume is large. A theory of collision for macroscopic viscoelastic spheres with the JKR interaction has been recently developed [9]. Besides the issue of how to describe grain-grain interactions during collision there is also the matter of the hardness of the material involved. At sufficiently high collision velocities, macroscopic elastic spheres tend to deform permanently leaving shallow indentations on their surfaces. The COR for these processes has long been shown to behave as $e \propto v_{\rm coll}^{-1/4}$ [10]. This result is also supported by experiments [11,12].

At the nanoparticle size-scale, recent studies on thin film deposition of nanoparticles on a substrate have revealed surprising collisional behavior. The experiments show that *slower moving nanoparticles can be more elastic with respect to a substrate than faster moving ones*. An intriguing feature of

*ytakato@buffalo.edu

very low velocity nanoparticle collisions reported recently in simulation-based studies is so-called "superelastic" collisions [13,14] where the grains can recoil at a slightly higher velocity than the original collision velocity. Such behavior is generally attributed to the conversion of some of the thermal vibrational energy into the kinetic energy of the center of mass. Large scale molecular dynamics (MD) simulations of the collision of two Lennard-Jones (LJ) nanoparticles were performed to examine their interaction force as well as their COR in collision regimes accompanied by elastic or small plastic deformations [15]. Although the MD-based interaction force between the two particles agrees with the corresponding JKR interaction force, the COR from the MD simulations is significantly lower than that from the JKR prediction due to the presence of additional energy dissipation mechanisms. At higher collision velocities these particles tend to soften and become more sticky [16,17]. The COR for these nanoparticles, as reported by Ayesh *et al*. [16], shows $v_{\rm coll}^{-1}$ dependence, which is attributed to extensive plastic deformation that extends through the whole nanoparticle. Our nonequilibrium MD-simulation-based study described below considers nanoparticles that range between small and those that are large enough to resemble very small elastic objects. As we shall see, the behavior of the COR found agrees with and extends upon the observations made by Ayesh *et al*. [16]. We observe that even the largest nanoparticles we can make are far too soft compared to the macroscopic grains probed via elasticity theory and this is why our studies do not recover the $v_{\rm coll}^{-1/4}$ dependence for the COR.

Yielding relates to the strength of a material. Hence one way of approaching the issue of how soft or hard these particles are is by focusing on the yield velocity. In the case of a material that experiences collision, the initiation of yielding, described by yield velocity, v_Y, is a material-dependent constant for macroscopic objects. As we shall see, yield velocity for our smallest nanoparticles (with 603 atoms) is much higher than that for bulk materials based on macroscopic theory [10], indicating that these particles can withstand larger velocity impacts before the initiation of yielding. The yield velocity for our nanoparticles has size dependence and approaches the macroscopic yield velocity as the size of the nanoparticle increases. The numerically obtained COR of Cu nanoparticles investigated by Han *et al*. [14] via MD seems to indicate a size dependence that is consistent with our finding.

Here, we report on collisions of two equal-sized nanoparticles composed of LJ atoms. We present the COR in terms of velocity ranging from as low as thermal velocity of atoms at the given temperature to velocity at which fragmentation of nanoparticles due to collision occurs. The yield of the particles is found to be particle size dependent. We shall also present evidence of distinctive permanent deformation modes for different collision velocities beyond the yield velocity. As we shall see, the overall trend of the COR in the range is described by the power law $e \sim v_{\rm coll}^{-1.03}$.

II. METHODS

In keeping with the literature [16] and for the sake of simplicity, we use the classical MD code LAMMPS, with the nanoparticles being approximate spheres of radius R made of 12-6 LJ atoms in a face-centered cubic (fcc) lattice structure. The atomic potential $V(r_{ij}) = 4\epsilon[(\sigma/r_{ij})^{12} - (\sigma/r_{ij})^{6}]$, where r_{ij} is an interatomic distance between atoms i and j. For argon, $\epsilon = 1.654 \times 10^{-21}$ J and $\sigma = 3.405$ Å and any values in SI units used in this paper are for argon. The radius and the number of atoms N in a particle range from $R =$ 1.73 nm, $N = 603$ to $R = 21.6$ nm, $N = 1\,072\,241$. We set the cutoff distance $r_c = 2.5\sigma$ for atoms belonging to the same nanoparticle and set $r_c = 2^{1/6}\sigma$ for any two atoms belonging to different nanoparticles to consider only repulsive interactions between the clusters. (Results obtained by simulations for $N = 5\,481$ with $r_c = 4\sigma$ and $r_c = 6\sigma$ for atoms within a particle agreed within the standard deviation.) The particle is not a perfect sphere because of the existence of facets arising from the underlying fcc structure. We placed two identical nanoparticles with facets facing each other. After creating the particles, they were equilibrated in a canonical ensemble (NVT) for more than 10 000 MD steps (time step $dt = 1.08 \times 10^{-14}$ s) to set their temperature $T = 2.396$ K ($=0.02\epsilon/k_B$), where k_B is the Boltzmann constant, using the Nosé-Hoover thermostat.

TABLE I. The system for simulations: R, cluster radius; N, number of atoms per cluster; and Runs, runs at the same velocity.

R (nm)	N	Runs	R (nm)	N	Runs
1.73	603	100	2.11	1 055	100
2.65	2 093	100	3.71	5 481	100
4.74	11 849	40	7.36	44 403	25
9.50	95 547	15	12.7	224 679	5
16.5	498 959	5	21.6	1 072 241	4

After the equilibration, we give equal and opposite center-of-mass velocities to the particles in order to make a head-on collision (see Fig. 3). During the collision process, we use microcanonical ensemble (NVE) simulations. The total energy of the system over the collision stage is conserved to around 10^{-5} in relative error. This is achieved for finite cutoffs by shifting the potential to zero at r_c. The collision velocity $v_{\rm coll}$ is varied from about 2 m/s (elastic collision regime) to 500 m/s (the maximum velocity at which clusters do not break into fragments due to collision). In order to quantify errors in calculated quantities, we perform multiple simulations in relatively small systems for each collision velocity by setting different initial thermal velocities. The systems and number of independent runs carried out for ensemble averaging are given in Table I.

III. RESULTS

Figure 1 shows the simulation results in terms of the COR for all cluster sizes and collision velocities. The COR of two nanoparticles was obtained by varying the collision velocity $v_{\rm coll}$ from 2.6 m/s ($0.016\sqrt{\epsilon/m}$) to 517 m/s ($3.29\sqrt{\epsilon/m}$) for each particle size N ranging from 603 to 1 072 241. For small collision velocities we find quasielastic collisions as seen in previous studies [13]. The COR for perfectly elastic collision is unity. Such an ideal collision is obtained, e.g., by using Hertzian spheres [5]. There is no energy dissipation during

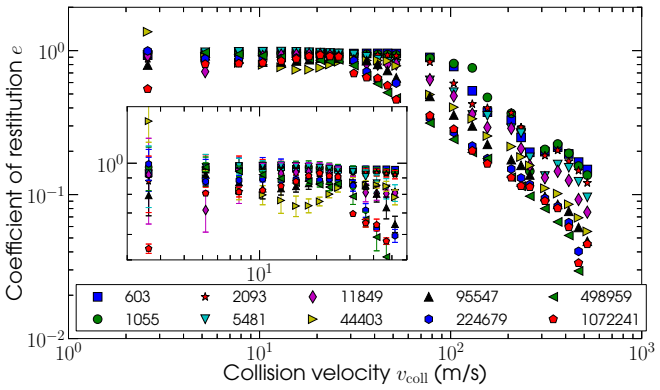

FIG. 1. (Color online) Coefficient of restitution between nanoparticles as a function of collision (relative) velocity. The onset of plastic deformation (yield) occurs at critical velocity corresponding to change in slope.

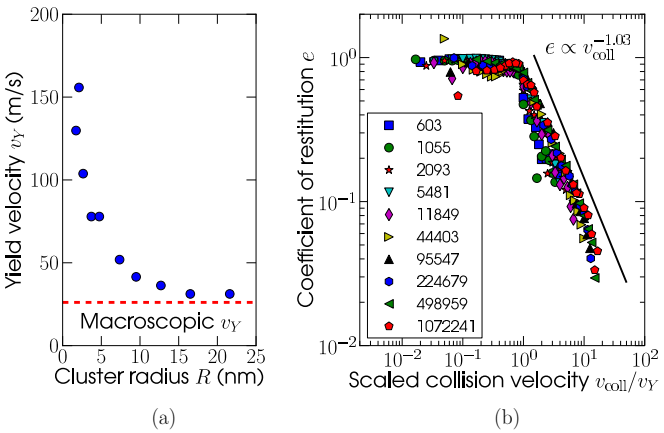

FIG. 2. (Color online) (a) Cluster-size dependence in yield velocity; (b) COR vs collision velocity rescaled by v_Y (line is a guide to the eye). The yield velocity for macroscopic spheres is shown as a dashed red line in panel (a).

collision; hence the center-of-mass kinetic energy in the system is conserved before and after collision. Figure 1 shows that the COR for small collision velocities is close to but less than unity. At the lowest collision velocities the spread in the data between runs gets larger due to thermal effects. This is especially so for smaller particles. In fact, for some of the smallest clusters, the COR exceeds unity, a behavior extensively reported on in Refs. [13,14]. While it may appear from the center-of-mass velocities of the particles that the particles gain kinetic energy from internal energy [13,14], in fact, as noted in previous studies, what actually occurs here is that the thermal fluctuations or the collective oscillations due to thermal fluctuations give an extra "kick" to the center-of-mass velocities of the recoiling nanoparticles. As the collision velocity is increased, the COR stays around unity and then shows a well-defined "kink" and falls roughly as a power law in the collision velocity. Moreover, the power law appears to be the same for all particle sizes. The data can be collapsed by taking the collision velocity where the kink occurs to be the yield velocity, v_Y, and then by rescaling each particle size's data by its v_Y. The velocity where the kink occurs is indeed the velocity where the onset of plastic deformation can be directly visualized, for example, by noting that just past this value a dislocation surface can be found to propagate through the particle as seen in Figs. 3(a) and 4(a). Hence, above this critical velocity lies the plastic or inelastic collision regime defined by the permanent deformation observed after collision.

The yield velocities for each nanoparticle size are plotted versus the particle size in Fig. 2(a). Rescaling the velocity of each particle size's data by its corresponding yield velocity produces a collapse of all the data as shown in Fig. 2(b); showing that the power-law decay of the COR is common to each nanoparticle size. It is remarkable that even though the deformation modes can be seen to be quite different depending on the collision velocity range, the slope of the COR follows a constant scaling with the collision velocity. The COR in the plastic deformation regime follows the approximate power law

$$e \propto v_{\mathrm{coll}}^{-1.03}. \qquad (1)$$

For macroscopic spheres, the COR for inelastic collisions which cause a shallow indentation on a spherical surface is $e \propto v_{\mathrm{coll}}^{-1/4}$ [10]. This has also been confirmed experimentally [11]. Our simulation results in Fig. 2(b) suggest that the COR decays with a slope of -1.03 for N between 2093 and 1 072 241. The value of the exponent obtained here agrees remarkably well with the recent work of Ayesh *et al.* [16]. Their experimentally and numerically obtained coefficient of normal restitution for nanoparticles that collide on a V-grooved surface at some incident angles shows v_{coll}^{-1} dependence in the strong plastic collision regime. Note that the coefficient of normal restitution in Ref. [16] is defined as the ratio of postcollision and precollision velocity components perpendicular to the surface. According to Ref. [18], oblique collisions associated with the change of normal direction between particles before and after collision may lower the COR. However it is not the case here since the normal direction between the nanoparticle and the surface remains the same. In contrast, our exponent α in Eq. (1) is larger than that of continuum theories, and hence the kinetic energy "loss" seen in nanoparticle collisions is much higher than that for the very gentle collisions of macroscopic grains. We have carried out preliminary studies on the velocity dependence of COR for 9-6 LJ potentials. Our results suggest α is within 2% of that reported here for the 12-6 LJ potential.

The difference between the two may be due to deformation modes: the deformation of particles here is large even at the onset of the plastic deformation [see Figs. 3(a) and 4(a)], whereas the deformation considered for macroscopic theories is limited to the vicinity of the contact surface of the two spheres. The work done to glide part of a nanoparticle along a lattice plane and to deform the whole nanoparticle along multiple planes as shown in Fig. 3 is expected to significantly exceed that needed to make a shallow indentation, and we believe that this difference leads to a lower COR for the nanoparticles. This lower COR implies that nanoparticles at high collision velocity are softer than macroscopic spheres and could hence be stickier due to the higher energy absorption due to the extensive particle deformation.

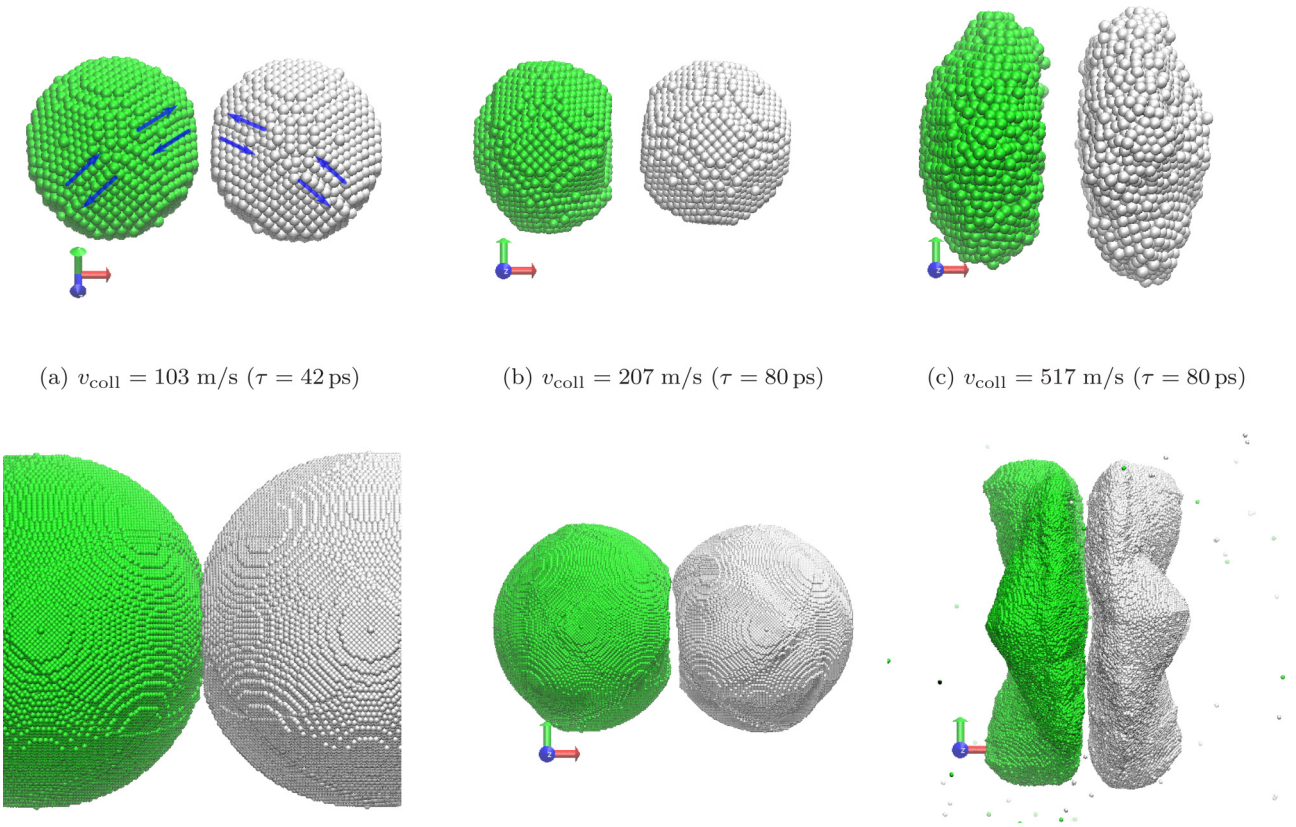

(a) $v_{\mathrm{coll}} = 103$ m/s ($\tau = 42$ ps) (b) $v_{\mathrm{coll}} = 207$ m/s ($\tau = 80$ ps) (c) $v_{\mathrm{coll}} = 517$ m/s ($\tau = 80$ ps)

(d) $v_{\mathrm{coll}} = 77.6$ m/s ($\tau = 147$ ps) (e) $v_{\mathrm{coll}} = 155$ m/s ($\tau = 212$ ps) (f) $v_{\mathrm{coll}} = 517$ m/s ($\tau = 244$ ps)

FIG. 3. (Color online) Deformation modes of two different nanoparticles: (a)–(c) $N = 5481$; (d)–(f) $N = 498\,959$. The snapshots here were taken at time τ ($\tau = 0$ when the nanoparticles come in contact.).

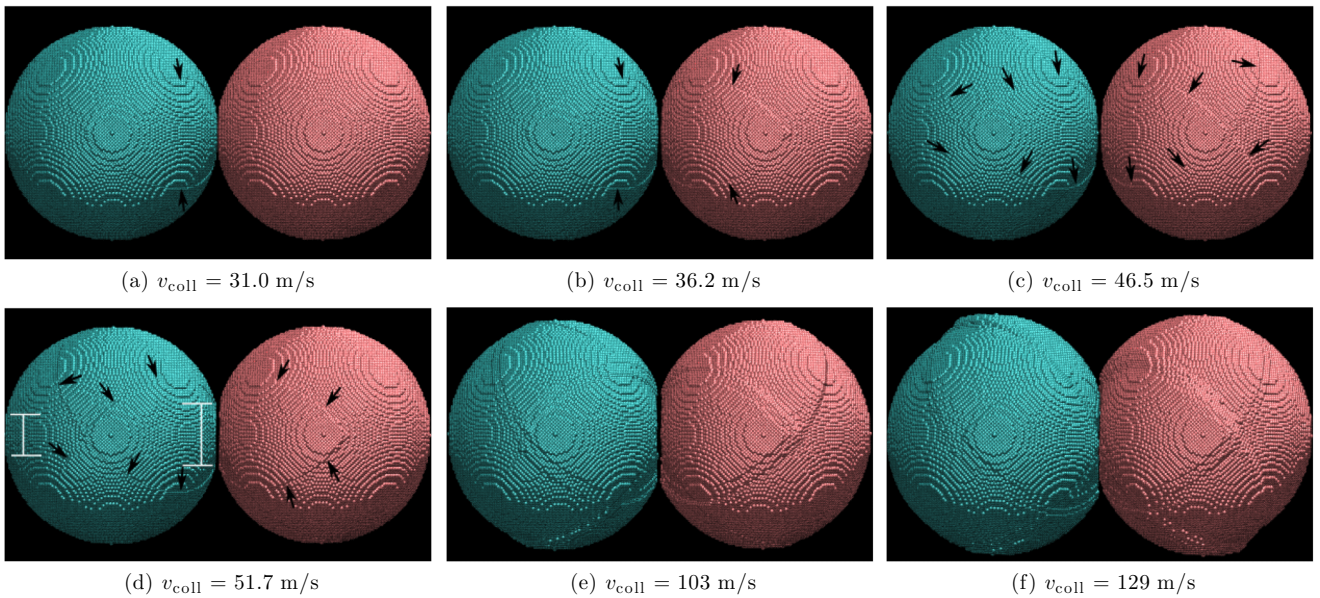

(a) $v_{\mathrm{coll}} = 31.0$ m/s (b) $v_{\mathrm{coll}} = 36.2$ m/s (c) $v_{\mathrm{coll}} = 46.5$ m/s

(d) $v_{\mathrm{coll}} = 51.7$ m/s (e) $v_{\mathrm{coll}} = 103$ m/s (f) $v_{\mathrm{coll}} = 129$ m/s

FIG. 4. (Color online) Dislocations in the $N = 498\,959$ particles above the critical velocity v_Y. In all cases $\tau = 180$ ps. The onset of permanent deformation is observed in panel (a). The two dislocation planes observed on the surface of the left particle in panel (a) reach the center of the projected surface approximately 90° apart from the contact surface. The number of dislocations increases progressively as the collision velocity gets higher [see panels (a)–(d)]. A large indentation at the contact surface is seen in panels (d)–(f). Dislocations occur as bands of slip lattice planes shown in panels (e) and (f), which result in the distorted spheres.

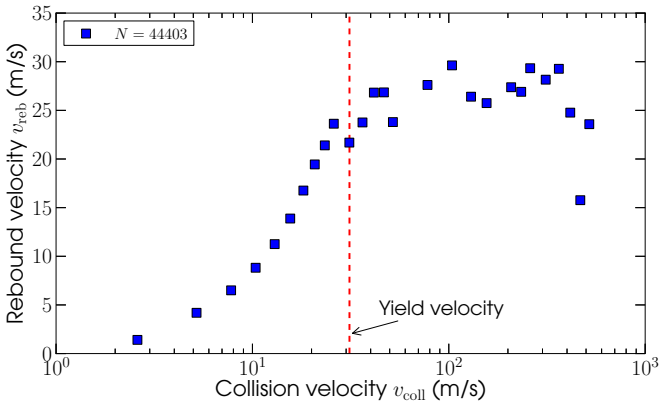

FIG. 5. (Color online) The rebound velocity v_{reb} is independent of the collision velocity v_{coll} above the yield velocity v_Y.

The power law in Eq. (1) indicates an important dynamical property regarding inelastic collisions. The rebound velocity v_{reb} of the nanoparticles is *independent* of the collision velocity since a comparison between the definition of COR $e \equiv v_{reb}/v_{coll}$ and our COR $e \propto v_{coll}^{-1.03}$ in the plastic collision regime leads to an approximately constant rebound velocity, v_{reb}. This independence is verified by the approximately flat region of the rebound velocity above the yield velocity as shown in Fig. 5. It also means the rebound kinetic energy remains the same regardless of how fast the nanoparticles collide. Therefore the entire amount of initial kinetic energy that is gained from the elastic collision regime, i.e., from just below v_Y, is transformed into their internal energy, e.g., permanent deformation and thermal energies as the snapshots of severely deformed nanoparticles are illustrated in Figs. 3 and 4.

Note that at some high collision velocities atoms were ejected from the clusters [see Fig. 3(f)]. This ejection due to massive collision energy occurred in nanoparticles that are for $N \geqslant 44\,403$. The kinetic energy of the ejected atoms is less than 0.2%. Hence ejected atoms do not influence the COR results reported here.

It is indicated above that the onset of plastic deformation depends on the cluster size. This is in contrast with the theory for macroscopic spheres due to Johnson [10] which predicts a size-independent yield velocity. According to the theory, the yield velocity v_Y is described by

$$\frac{1}{2}M^* v_Y^2 = \frac{53R^{*3}Y^5}{E^{*4}}, \tag{2}$$

where reduced mass $M^* = M/2$ obtained from mass of a cluster M, reduced radius $R^* = R/2$, Y is the yield strength, and reduced Young's modulus $E^* = E/[2(1-\nu^2)]$, defined with Poisson's ratio ν. The theoretical yield stress for an ideal fcc lattice is given by $Y \simeq G/10$, where G is the shear modulus. Quesnel *et al.* [19] determined Young's modulus, Poisson's ratio, and shear modulus in the [100] direction for the fcc LJ solid using MD. Their values $E = 61.1\epsilon/\sigma^3$, $G = 57.2\epsilon/\sigma^3$, and $\nu = 0.347$ give the yield velocity to be 26.1 m/s for our nanoparticles when colliding in the [100] direction.

In the MD simulations, as the particle size increases, the onset of plastic deformation occurs at progressively lower collision velocities. That the yield velocity shifts lower as the cluster size increases implies that larger clusters yield more easily. This was observed in MD simulations of collisions of a Cu cluster with a surface by Han *et al.* [14]. In an experimental study of collisions of an ice cluster on an ice block, Higa *et al.* [20] reported size dependence of the yield velocity $v_Y \propto R^{-0.5}$. It would seem, however, that the yield velocity should be a size-independent constant for macroscopic spheres since the ratio of the number of atoms in a cluster and the radius of a cluster, N/R, remains unchanged. Figure 2(a) displays a clear size dependence which appears to approach a value near the approximated macroscopic value as the particle size increases (26.1 m/s, drawn as a dashed red line in the same figure). A shear MD simulation study by Horstemeyer *et al.* [21] on nano-sized blocks of fcc metal revealed the size dependence of the yield strength at a low strain rate. Their yield strength was found to be proportional to $d^{-0.25}$, where d is the block size. This power law leads to the size-dependent yield velocity $v_Y \propto R^{-0.625} \approx R^{-0.63}$ of a macroscopic sphere by assuming $Y \propto R^{-0.25}$ in Eq. (2). It gives a fair agreement with our nanoparticles' yield velocity $v_Y \propto R^{-0.65}$. That said, further simulations for larger particle sizes would be desirable to confirm our understanding.

IV. CONCLUSION

We have studied MD-simulation-based collisions of argon nanoparticles with appropriate LJ interactions between the atoms. The clusters range in size from 603 to 1 072 241 atoms each. We find that at sufficiently low collision velocities the superelastic effects seen in Refs. [13,14] are observed; below the yield velocity COR ~ 1, whereas above the yield velocity COR $\sim v_{coll}^{-1.03}$, the latter result being consistent with the MD-based (but much smaller systems) studies and experiments in Ref. [16]. In addition, we find that the yield velocity shows the power-law dependence in nanoparticle size and approaches the constant value by the continuum theory as the nanoparticle radius increases. Nanoparticles are harder and highly elastic at $v_{coll} < v_Y$ and progressively soften owing to significant structural changes for $v_{coll} > v_Y$, a phenomenon that is consistent with the recent experimental observations of Ayesh *et al.* [16]. The softness and stickiness of fast moving nanoparticles could be beneficial in many applications, for instance, a process of nanoparticle coating by the laser ablation on a substrate in a vacuum chamber for a more efficient method.

ACKNOWLEDGMENTS

Y.T. and S.S. were supported by US Army Research Office. Sandia National Laboratories is a multi-program laboratory managed and operated by Sandia Corporation, a wholly owned subsidiary of Lockheed Martin Corporation, for the U.S. Department of Energy's National Nuclear Security Administration under contract DE-AC04-94AL85000. The authors thank Mr. Michael Benson for carrying out some of the simulations for the 9-6 LJ potential.

[1] G. Barnes, Am. J. Phys. **26**, 5 (1958).
[2] H. Arastoopour, Powder Technol. **119**, 59 (2001).
[3] P. Goldreich and W. R. Ward, Astrophys. J. **183**, 1051 (1973); K. Wada, H. Tanaka, T. Suyama, H. Kimura, and T. Yamamoto, *ibid.* **661**, 320 (2007).
[4] S. Rajagopalachary, S. V. Verkhoturov, and E. A. Schweikert, Nano Lett. **8**, 1076 (2008).
[5] H. Hertz, J. Reine Angew. Math. **92**, 156 (1881); D. Sun, C. Daraio, and S. Sen, Phys. Rev. E **83**, 066605 (2011).
[6] G. Kuwabara and K. Kono, Jpn. J. Appl. Phys. **26**, 1230 (1987).
[7] J.-M. Hertzsch, F. Spahn, and N. V. Brilliantov, J. Phys. II **5**, 1725 (1995); N. V. Brilliantov, F. Spahn, J. M. Hertzsch, and T. Pöschel, Phys. Rev. E **53**, 5382 (1996); R. Ramirez, T. Pöschel, N. V. Brilliantov, and T. Schwager, *ibid.* **60**, 4465 (1999); S. Antonyuk, S. Heinrich, J. Tomas, N. G. Deen, M. S. van Buijtenen, and J. A. M. Kuipers, Granular Matter **12**, 15 (2010).
[8] K. L. Johnson, K. Kendall, and A. D. Roberts, Proc. R. Soc. London, Ser. A **324**, 301 (1971).
[9] N. V. Brilliantov, N. Albers, F. Spahn, and T. Pöschel, Phys. Rev. E **76**, 051302 (2007).
[10] K. L. Johnson, *Contact Mechanics* (Cambridge University Press, Cambridge, UK, 1987); C. Thornton, J. Appl. Mech. **64**, 383 (1997); C. Thornton and Z. Ning, Powder Technol. **99**, 154 (1998).
[11] L. Labous, A. D. Rosato, and R. N. Dave, Phys. Rev. E **56**, 5717 (1997).
[12] A. H. Kharaz and D. A. Gorham, Philos. Mag. Lett. **80**, 549 (2000).
[13] H. Kuninaka and H. Hayakawa, Prog. Theor. Phys. Suppl. **178**, 157 (2009); Phys. Rev. E **79**, 031309 (2009).
[14] L. B. Han, Q. An, S. N. Luo, and W. A. Goddard III, Mater. Lett. **64**, 2230 (2010).
[15] H. Tanaka, K. Wada, T. Suyama, and S. Okuzumi, Prog. Theor. Phys. Suppl. **195**, 101 (2012).
[16] A. I. Ayesh, S. A. Brown, A. Awasthi, S. C. Hendy, P. Y. Convers, and K. Nichol, Phys. Rev. B **81**, 195422 (2010).
[17] A. Awasthi, S. C. Hendy, P. Zoontjens, and S. A. Brown, Phys. Rev. Lett. **97**, 186103 (2006); A. Awasthi, S. C. Hendy, P. Zoontjens, S. A. Brown, and F. Natali, Phys. Rev. B **76**, 115437 (2007).
[18] K. Saitoh, A. Bodrova, H. Hayakawa, and N. V. Brilliantov, Phys. Rev. Lett. **105**, 238001 (2010); P. Müller, D. Krengel, and T. Pöschel, Phys. Rev. E **85**, 041306 (2012).
[19] D. J. Quesnel, D. S. Rimai, and L. P. DeMejo, Phys. Rev. B **48**, 6795 (1993).
[20] M. Higa, M. Arakawa, and N. Maeno, Icarus **133**, 310 (1998).
[21] M. F. Horstemeyer, M. I. Baskes, and S. J. Plimpton, Acta Mater. **49**, 4363 (2001); Theor. Appl. Fract. Mech. **37**, 49 (2001).